Voltammetric Studies of the Redox Polymer Poly[4,4′-bipyridinium-1,1′-diylcarbonyl-2,5-thiophenediyl Dichloride] in Dimethyl Sulfoxide

Bhim Bali PRASAD* and Sandhya SINGH
Analytical Division, Chemistry Department, Faculty of Science, Banaras Hindu University, Varanasi-221005, India
(Received May 2, 1994)

The electrochemical behavior of a redox polyelectrolyte, poly[4,4′-bipyridinium-1,1′-diylcarbonyl-2,5-thiophenediyl dichloride] at mercury electrode has been examined in dimethyl sulfoxide containing different concentrations of tetrabutylammonium iodide. The techniques of sampled DC polarography, pulse polarography (normal and differential), and cyclic voltammetry have been used. All polarograms revealed three one-electron reduction waves which are found either quasi-reversible or irreversible and usually adsorption-controlled by cyclic voltammetric experiments. The results were discussed by taking into account the implications of different concentrations of supporting electrolytes and polycation conformations on the adsorption processes consisting of preceding and following chemical reactions coupled with charge transfer reactions occurring at the electrode.

In the quest to explore viologen chemistry[1] polarographically, some interesting investigations of redox polyviologens containing *o*-, *m*-, and *p*-phenylenebis(methylene) (–CH_2–⟨⟩–CH_2–), ethylene (–CH_2–CH_2–) and *N*-oxyxylylene (–N–O–CH_2–⟨⟩–CH_2–) linkages in their polymeric network have been undertaken from our laboratory,[2a,2b,2c,2d,2e,2f] where electroactive viologen (4,4′-bipyridinium) units are interspersed with electro-inactive α,ω-dihalogen compounds such as α,α'-dibromo-(*o*,*m*,*p*)-xylene, 1,2-dibromoethylene; etc. However, polyviologens, in which both the substituents are electroactive and which can have a mutual effect on the electron-transfer properties, have not hitherto received any attention. Thus, the present paper deals with the electrochemistry of such polyviologen namely, poly[4,4′-bipyridinium-1,1′-diylcarbonyl-2,5-thiophenediyl dichloride] ($PTVCl_2$) in dimethyl sulfoxide (DMSO) at mercury electrode employing various modern voltammetric techniques. $PTVCl_2$ (as shown by the Chart 1. Structure 1) has been reportedly stable oligomer, with *N*-acylammonium-type linkages between bipyridinium and thiophenediyl moieties in the parent chain, through the resonance stabilized intramolecular electrostatic bonding.[3] The particular surge of interest in DMSO is due to its dipolar aprotic nature which may apparently bring upon the distinctive ion-solvent dipole interactions, and thereby conformation alternations of the polymer in dilute solution of different ionic strengths. This may lead to an interesting study of the polymer at electrode–electrolyte interface, while deliberately keeping the effects of migration currents and iR compensations at extremely low electrolyte concentrations in abeyance (cf. subsequent discussion).

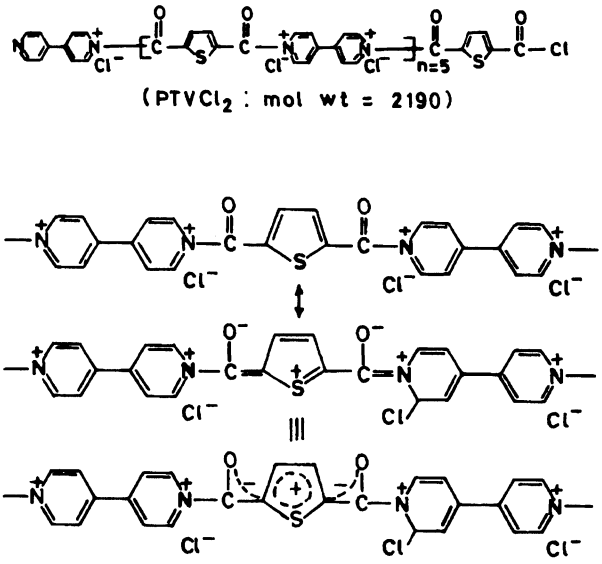

Chart 1.

Experimental

Materials. Dimethyl sulfoxide (E. Merck, India) was dried over 5 Å molecular sieves and distilled under reduced pressure at 80 °C at about 10—15 Torr (1 Torr=133.322 Pa). Specific conductivities of purified solvent ranged between 1.0×10^{-8} and 2.0×10^{-8} S cm^{-1} at 25 °C. Karl Fischer titration failed to detect any water in the solvent DMSO as it was well protected in an automatic dispensor under nitrogen gas atmosphere to avoid any moisture exposure. Anhydrous tetrabutylammonium iodide (TBAI) (Sigma) was used as supporting electrolyte without any further purification.

The preparation and characterization of the poly viologen-containing polymer $PTVCl_2$ (M_w 2190) was followed according to the earlier recipe.[3] All other chemicals were of analytical grade.

Methods. All the voltammograms (sampled DC polarography (DCP- Tast), Normal pulse polarography (NPP), Differential pulse polarography (DPP), and Cyclic voltammetry (CV) were recorded in the manner reported elsewhere,[2d] at room temperature (ca. 25 °C) with the help of PAR 264A Voltammetric Analyzer in conjunction with PAR 303 SMDE stand consisting of a mercury electrode (HMDE, SMDE, DME modes), a platinum wire auxillary electrodes, and an Ag/AgCl (sat KCl in nonaqueous filling solution) reference electrode. Typical parameters employed were: drop time 1 s, scan rate (v) 5 mV s^{-1}, modulation amplitude 25 mV.

During coulometric measurements and controlled poten-

Table 1. Summary of Results of Voltammetric Measurements (DCP-tast, NPP, DPP) of 0.390 g dm^{-3} $PTVCl_2$ in DMSO at 25 °C[a,b]

Concn [TBAI]		Wave I					Wave II					Wave III				
M		i_l	$E_{1/2}$	α_n	n	$\omega_{1/2}$	i_l	$E_{1/2}$	α_n	n	$\omega_{1/2}$	i_l	$E_{1/2}$	α_n	n	$\omega_{1/2}$
0.0013	DCP-Tast	2.50	−0.750	0.57	0.62	—	2.80	−0.965	0.74	0.80	—	3.30	−1.485	0.35	0.38	—
	NPP	3.50	—	—	—	—	12.50	−0.925	—	—	—	15.00	−1.375	—	—	—
	DPP	3.25	−0.775[c]	—	—	—	5.75	−1.020[c]	—	—	—	4.25	−1.550[c]	0.23	—	−0.36
0.100	DCP-Tast	0.56	−0.850	0.74	0.80	—	0.82	−1.495	0.36	0.38	—	—	—	—	—	—
	NPP	2.10	−0.850	—	—	—	2.90	−1.525	—	—	—	3.10	−2.060	—	—	—
	DPP	2.45	−0.850[c]	0.72	—	−0.115	2.55	−1.50[c]	0.39	—	0.21	2.65	−2.050[c]	0.59	—	−0.14

a) Units: i_l=limiting current (μA); $E_{1/2}$=half-wave potential (V vs. Ag/AgCl); α_n and n=parameters derived from Tomes criterion); $\omega_{1/2}$=half peak with in V vs. Ag/AgCl. b) Blanks show not-workable data. c) E_s (summit potential) in V vs. Ag/AgCl.

tial electrochemical reduction in thermostated two compartmental cell containing 5 ml of $PTVCl_2$ in 0.1 M (M= mol dm^{-3}) TBAI in DMSO, a mercury pool cathode (area 3.5 cm^2) is maintained at the potential 3.0 V vs. SCE. A relatively slow stirring of the mercury pool is particularly required at the outset of electrolysis because the adsorption phenomenon causes the partition of mercury cathode into small balls isolated from each other by the adsorbed film. No reduction products were identified in the solution. The cation radicals formed, as evident from brownish color over droplets, however, may be apparently oxidized at anode by the iodine liberated and get discolored. Nevertheless, the colorless residue obtained from removal of solvent is subjected to IR analysis for further identification.

Results and Discussion

Sampled DC Polarography. Typical DCP-tast curves of $PTVCl_2$ in DMSO solutions at different concentrations of supporting electrolyte (TBAI) are shown in Fig. 1. The results obtained from the analysis of current-potential DCP-tast curves particularly at two concentrations of supporting electrolytes are summarized in Table 1. As is evident from analysis of results (Fig. 1a and Table 1), the DCP-tast curves were observed to be drastically influenced by the concentration of supporting electrolyte. For all solutions studied two well-defined (I & II) were obtained along with wave III which in dilute solution (<0.0013 M) of supporting electrolyte is relatively readily obtained and defined than that in higher concentration (0.1 M) of TBAI. It should be further noted from Table 1 that the relative wave heights for waves I and II are drastically reduced and respective half-wave potentials were negatively shifted in the case with 0.1 M TBAI as compared to 0.0013 M TBAI for the concentration of 0.39 g dm^{-3} of the depolarizer. This shows a modest contribution of charge transport via migration or uncompensated resistance at very low electrolyte concentration, while on the other hand, the major reduction in current at higher concentration of background electrolyte indicates probably a restricted mode of reduction owing to the higher ionic strength of tetrabutylammonium ions (TBA^+) in the vicinity of the cathode which presumably repell the polycations from the bulk of diffusion layer into the bulk of the

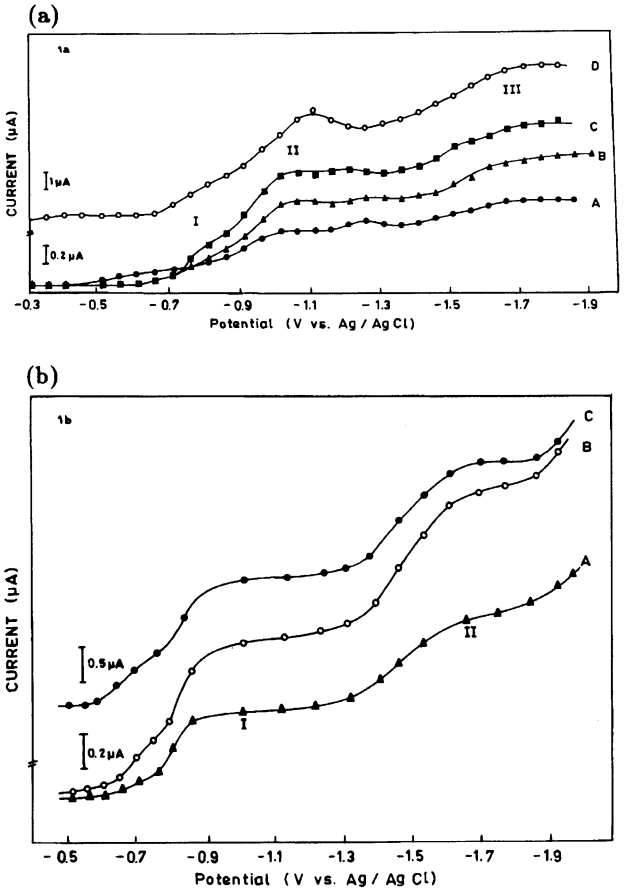

Fig. 1. (a) DCP- tast polarograms of $PTVCl_2$ in DMSO at concentrations: A, 0.043 g dm^{-3} (0.2×10^{-3} M TBAI); B, 0.078 g dm^{-3} (0.3×10^{-3} M TBAI); C, 0.106 g dm^{-3} (0.4×10^{-3} M TBAI); D, 0.390 g dm^{-3} (1.3×10^{-3} M TBAI). (b) DCP-tast polarograms of $PTVCl_2$ in DMSO at concentrations: A, 0.21 g dm^{-3}, B, 0.39 g dm^{-3} and C, 0.63 g dm^{-3} in 0.1 M TBAI as supporting electrolyte, perturbed wave III is not shown.

solution. The ion-pair formation of cation sites of depolarizer in concentrated TBAI could be also another reason for lessened reduction and negative shift in $E_{1/2}$ values. The emergence of a pre-wave to wave I in concentrated medium of supporting electrolyte reflects the

adsorption of reduction product of wave I which undergoes further reduction into wave II with a corresponding post-wave, while perturbed or ill-defined nature of wave III at higher negative potentials is probably due to electrode perturbations caused by the adsorption of TBA^+ ions (Fig. 1b). The i_l vs. C plots for waves I, II, and III show nonlinearity in dilute ranges of depolarizer and supporting electrolyte concentrations, whereas the same for I and II waves show reasonably linear nature and diffusion-controlled electron-transfer behavior at all concentrations of $PTVCl_2$ in 0.1 M TBAI solutions. In the dilute ranges of $PTVCl_2$ and TBAI concentrations, the quaternary centres of molecular chain, which can easily resume stabilization as PTVCl through partial dissociation of Cl^- in lower permittivity of DMSO, have interionic repulsions and thereby extended conformation. This promotes adsorbed layer of depolarizer over Hg drops surface causing a deviation from linearity in i_l vs. C plots in low electrolyte concentration. On the other hand, the insignificant adsorption in the presence of higher concentration of background electrolyte is simply because of the fact that the intramolecular charge interactions in $PTVCl_2$ and/or the pre-emption of adsorption sites of the background electrolyte compete with the adsorption of $PTVCl_2$.[2g]

On application of $E_{3/4}$ and $E_{1/4}$ values, as obtained from all waves at concentration 0.39 g dm^{-3}, in the following Tomes criterion of a reversible (Eq. 1) and irreversible waves (Eq. 2),

$$E_{3/4} - E_{1/4} = \frac{-0.0564}{n} \quad (1)$$

$$E_{3/4} - E_{1/4} = \frac{-0.05172}{\alpha_n}, \quad (2)$$

the values of n and α_n are calculated as given in Table 1. Although practically no dependence of $E_{1/2}$ values on concentration is observable (Fig. 1) at a particular ionic strength of supporting electrolyte, the fractional values of α_n and n still appear to be reasonable and in conformity with the irreversible nature of electrode process in sampled DC polarography.

The total number of electrons (n) involved in the complete reduction of $PTVCl_2$ was obtained as 3.0 by the help of a microscale coulometric experiment. This could be apportioned between all three waves suggesting one electron per reduction. A probable mechanism of electron-transfer reactions can be suggested by keeping in view the $\rangle$N=C bond of the first regularly quaternized center of the terminal bipyridine ring is less accessible to reduction since the positive charge density of the concerned quaternary center is presumably shielded by the terminal unshared nitrogen's electron pair and adjacent anion of neighboring acyl group interacting with it.[2b] Furthermore, *N*-acyl group is reported[4] to remain intact during reduction. Under such circumstances, the first and second reductions are believed to occur with one electron involvement in the vicinity of the next quaternary centers[2b] other than terminal positive nitrogen of the molecule. Thus the system may undergo three successive reduction steps producing cationic mono-, di-, and tri-radicals (Chart 2. Structure 2). Although it is difficult to provide an experimental evidence of reduction mode(s) because of very limited stability of radicals so produced. However, the tentative assignment of reduction sites could be possible by assuming that the associated chlorine would exert an electron-withdrawing effect making the adjacent $\rangle\overset{+}{N}$= centers more electron deficient than the other quaternary centers; $-\overset{+}{S}$=C$\langle$ center is less reductive due to its charge delocalization under the influence of acyl moieties at 2,5-positions. Therefore, the first and second reductions occur at quaternary N^+ centers of $\rangle N^+$=$\overset{O^-}{\overset{|}{C}}$– bond and $\rangle\overset{+}{N}$=C bond of bipyridinium residue whereas the wave III is attributed to the reduction of $-\overset{+}{S}$=C$\langle$ bond of thiophenediyl moiety. The remarkable shift in reduction potential than monomer 1,1′-dialkyl-4,4′-bipyridinium compound may be attributed to cannonical structure of *N*-acyl iminium linkages (Chart 1. Structure 1). It is interesting to note that the triradical dianionic reduction product (PTV···) may demonstrate electrostatic bonding with TBA^+ ions as well as enhanced solvophobic interactions with DMSO molecules resulting in an apparent solvent structuring and perturbed double layer around the electrode surface. This is why we observed at random fall of Hg droplets and extensive capillary

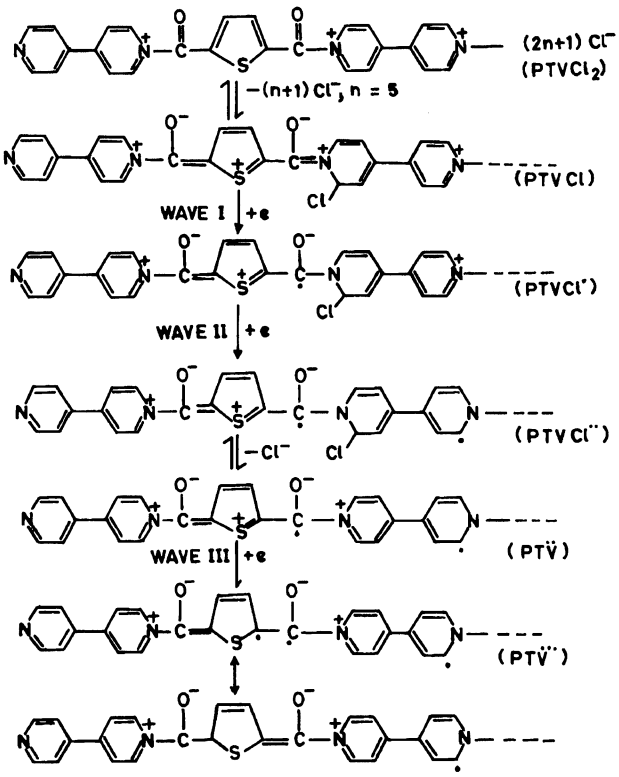

Chart 2.

noise while recording wave III at higher negative potential in the concentrated medium of the supporting electrolyte. The IR analysis of the residue obtained after complete reduction gave all frequencies similar to those obtained for original compound. However, the $\rangle C{=}O$ stretching frequency (1780 cm^{-1}) is found to be shielded to 1037 cm^{-1} owing to the reduction into $\rangle C{-}O^-$ group. This is in support of the proposed mechanism of electroreduction.

Pulse Polarography. Typical NPP and DPP runs for 0.39 $g\,dm^{-3}$ $PTVCl_2$ in both ranges of TBAI concentration (0.0013 M and 0.1 M) are shown in Figs. 2a and 2b. The reduction in current for all waves in concentrated supporting electrolyte medium is also observed like DCP-tast. Half-wave potentials of all NPP waves are consistent with their corresponding values in DCP-tast. However, the third wave and pre-peak to the first wave is clearly resolved in DPP as compared to NPP. From the treatment suggested by Oldham and Parry[5] as the 7:1 ratio of wave heights of NPP cathodic and anodic waves for irreversible process and 1:1 ratio for reversible reduction are indicative of the type of process occurring, $\frac{i_l\ (\text{cathodic})}{i_l\ (\text{anodic})}$ values [wave I (0.6), wave II (1.4), and wave III (4.0)] calculated for the solution of 0.39 $g\,dm^{-3}$ $PTVCl_2$ in 0.0013 M TBAI in

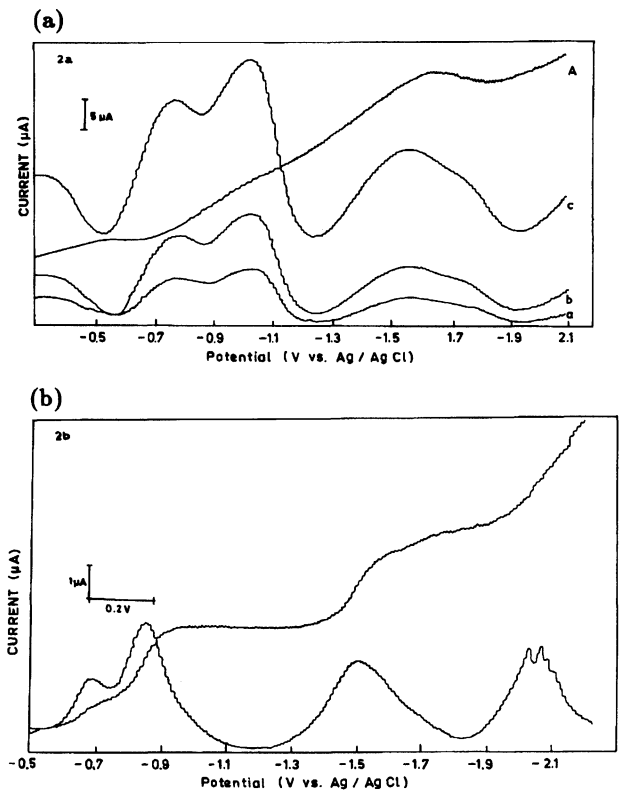

Fig. 2. (a) NPP and DPP runs of $PTVCl_2$ in DMSO at concentration 0.39 $g\,dm^{-3}$ (1.3×10^{-3} M TBAI) 'a', 'b', 'c' are DPP with pulse heights 25, 50, and 100 mV, respectively and 'A' is NPP). (b) NPP and DPP runs of $PTVCl_2$ in DMSO at concentration 0.39 $g\,dm^{-3}$ (0.1 M TBAI).

the present instance accordingly indicate the reversible behavior of the second reduction and the irreversible nature of waves I and III waves in NPP mode. This shows fast electrode kinetics of wave II within the small time ($\tau-\tau'=17$ ms) of pulse than conventional polarographic experiment ($\tau=1$ s). Other waves have sluggish irreversible electrode kinetics. The ratio of reversible current in normal pulse mode to tast mode for wave II is 4.6 (0.0013 M TBAI), while that calculated by i_d pulse/i_d tast$=(3/7)^{1/2}(\tau/\tau-\tau')^{1/2}$ is 5.0 which is in fair agreement[6] despite the less reversibility ($n=0.80$) of respective tast polarograms. This shows that the degree of reversibility of wave II in DCP-tast mode is disrupted not solely due to the slow electron transfer but due to the possibility of coupled chemical reaction following charge transfer ($PTVCl^{\bullet\bullet}\rightleftharpoons PTV^{\bullet\bullet}+Cl^-$) also. This was confirmed later by cyclic voltammetry. In Fig. 2b all waves were well-resolved in concentrated supporting electrolyte showing also a pre-peak to the wave I and a post-peak drawn out at the foot of the wave II. This shows adsorption complications due to the adsorption of the first reduction product ($PTVCl^{\bullet}$) which is also a successive reactant for the second wave in both concentrations of the supporting electrolyte (cf. Fig. 1a). The determination of half peak width ($\omega_{1/2}$) obtained from $\omega_{1/2}=3.25RT/\alpha_{nF}$ is not workable because of successive asymmetrical DPP peaks. However, in some cases they could be estimated as greater than 120 mV (Table 1) which are much higher than those corresponding to the reversible wave.[7] The corresponding fractional values of α_n denote irreversible behavior of all the three waves. From the relationship relating the peak potential (E_s) and half-wave potential ($E_{1/2}$),[6]

$$E_{1/2} = E_s + \Delta E/2, \tag{3}$$

where ΔE is a small pulse amplitude (25 mV), $E_{1/2}$ values were found to have practically good agreement with those determined by DCP-tast or CV (In CV, $E_{1/2}$ is equivalent of the average of E_{pc} and E_{pa}). Since ΔE is small, the potential of maximum current (E_s) lies close to the polarographic half-wave potential. In spite of the fact that the time scale in DPP and NPP is identical, the appreciable degree of reversiblity of wave II in NPP is contrary to that observed in DPP. This may be due to the fact that the rising portion of wave II in DPP extends over larger potential range due to the strong adsorption of the reactant giving larger peak width and lower transfer coefficient (α). The DPP peak height was found increasing as the pulse height used larger in slightly nonlinear fashion (Fig. 2a). However, DPP peak current at 100 mV pulse amplitude for wave I and II was found surprisingly much larger than the Cottrell limit (NPP current) while wave III is within the limiting value (Fig. 2a). This may be due to the adsorption effects of electroactive materials associated with wave I and II which perhaps augment the current in DPP mode

Table 2. Cyclic Voltammetric Results for $PTVCl_2$ (0.39 g dm^{-3}) at Various Scan Rates in DMSO in Supporting Electrolyte TBAI (1.3×10^{-3} M)[a,b]

Scan rate[c]	Peak	E_{pc}	E_{pa}	E_p	I_{pc}	I_{pa}	I_{pa}/I_{pc}	$I_{pc}/v^{1/2}$	$I_{pc}/Cv^{1/2}$ [d]
0.050	1	−0.775	−0.650	−0.125	0.4	0.3	0.75	1.82	10.22
	2	−1.000	−0.825	−0.175	1.4	0.7	0.50	6.36	35.73
	3	−1.625	—	—	0.7	—	—	3.18	17.86
0.100	1	−0.775	−0.625	−0.150	0.5	0.4	0.80	1.61	9.04
	2	−1.035	−0.800	−0.235	1.9	0.8	0.42	6.13	34.43
	3	−1.700	—	—	0.8	—	—	2.58	14.49
0.200	1	−0.800	−0.585	−0.215	0.6	0.7	1.16	1.36	7.64
		(−0.850)	(−0.580)	(−0.270)	(0.5)	(0.9)	(1.8)	(1.14)	(6.40)
	2	−1.075	−0.775	−0.300	2.4	0.9	0.375	5.54	30.61
		(−1.09)	(−0.775)	(−0.315)	(2.6)	(1.0)	(0.38)	(5.91)	(33.20)
	3	−1.750	—	—	0.9	—	—	2.05	11.51

a) Units: I_{pc}=cathodic peak current (μA); I_{pa}=anodic peak current (μA); E_{pc}=cathodic peak potential (V); E_{pa}=anodic peak potential (V); $\Delta E_p=|E_{pc}-E_{pa}|$, v=scan rate (V s^{-1}). b) Blanks denote not-workable data. Values given in parentheses denote parameters when $E_\lambda=-1.5$ V vs. Ag/AgCl. c) Only middle scan rates data are given. d) C is mM (on the basis of the total average molecular weight of the oligomer).

over a greater range of pulse potential. The cathodic shifts in half wave potentials in DPP mode in 0.0013 M TBAI as compared to those in NPP mode, however, indicate a severe adsorption complication all along wide potential ramp (Fig. 2a).

Cyclic Voltammetry. The typical cyclic voltammograms recorded at various scan rates (v) with a triangular potential sweep from −0.30 to −1.9 V and back to −0.3 V vs. Ag/AgCl, at $PTVCl_2$ concentration of 0.39 g dm^{-3} show three major cathodic peaks i_{pc_1}, i_{pc_2}, and i_{pc_3} and two anodic peaks i_{pa_1} and i_{pa_2}, when supporting electrolyte TBAI concentration used was 0.0013 M (Fig. 3). However, the similar voltammograms of $PTVCl_2$ in 0.1 M TBAI gave three cathodic peaks i_{pc_1}, i_{pc_2}, and i_{pc_3} and two anodic peaks i_{pa_1} and i_{pa_3} in anodic scan (Fig. 4, CV only shown at v=0.200 V s^{-1}). In both concentrations of supporting electrolytes, peaks i_{pc_1} and i_{pa_2} are always preceded with an ill-defined 'reversible' pre-peak ($i_{pc'}$ and $i_{pa'}$), and the second peaks i_{pc_2} and i_{pa_2} are followed with a drawn out 'reversible' post-peaks ($i_{pc''}$ and $i_{pa''}$). The effect of switching potential ($E_\lambda=-1.5$ V) was studied for $PTVCl_2$ (concentration 0.39 g dm^{-3}) in dilute TBAI concentration (0.0013 M) which corresponded only first two peaks i_{pc_1}, i_{pa_1} and i_{pc_2}, i_{pa_2} in respective cathodic and anodic branches (Fig. 3). Tabulations of voltammetric parameters are made in Table 2.

The appearance of reversible pre-peaks as stated above indicates the strong adsorption of the product of the first reduction. Subsequently this causes an emergence of post-peak in its successive reduction corresponding to the second peak. The nonlinear behavior of I_p vs. $v^{1/2}$ and I_p vs. concentration [$PTVCl_2$] for all the peaks in both concentrations of supporting electrolyte also show the electrode perturbation by adsorption in agreement with conclusions reached for DCP-tast/pulse polarograms. Cathodic peak potentials of first and second peaks are found negatively shifting with scan rate whereas anodic peaks for first and second peaks are found to be slightly positively shifted with scan rate in the lower concentration of supporting electrolyte. In spite of the fact that peak potentials change with scan rate (a behavior expected in the case of irreversible process), peak separation ΔE_p (Table 2) in the present case is much more than what expected for (60 mV) a reversible one-electron process. This shows that

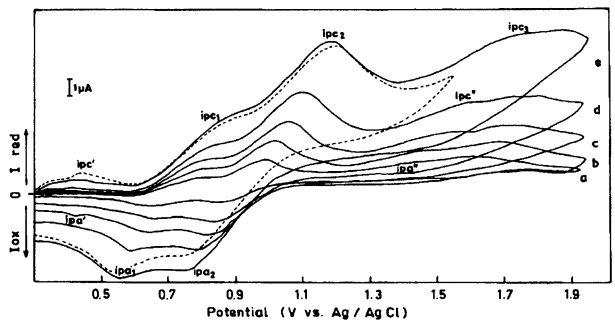

Fig. 3. Cyclic voltammograms of $PTVCl_2$ in DMSO at concentration 0.39 g dm^{-3} (1.3×10^{-3} M TBAI) at scan rates v (V s^{-1}): a, 0.020; b, 0.050; c, 0.100; d, 0.200; e, 0.500. Dotted run is CV at $E_\lambda=-1.5$ V and scan rate=0.500 V s^{-1}.

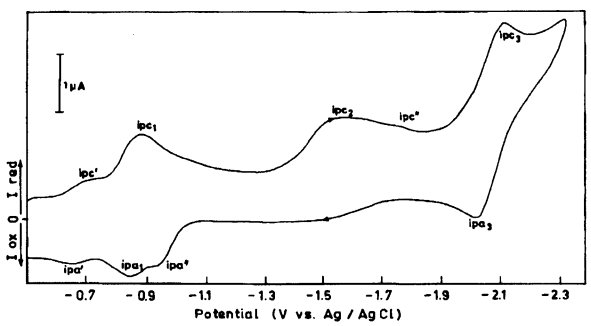

Fig. 4. Cyclic voltammograms of $PTVCl_2$ in DMSO at concentration 0.390 g dm^{-3} (0.1 M TBAI) at 0.200 V s^{-1} scan rate.

Table 3. Cyclic Voltammetric Results of $PTVCl_2$ at Scan Rate 0.200 $V s^{-1}$ in Supporting Electrolyte TBAI (0.1 M)[a,b]

Concentration [$PTVCl_2$] / g dm^{-3}	Peak	E_{pc}	E_{pa}	E_{pc}	I_{pc}	I_{pa}	I_{pa}/I_{pc}	$I_{pc}/v^{1/2}$	$I_{pc}/Cv^{1/2}$ [c]
0.21	1	−0.875	−0.835	−0.040	0.45	0.37_5	0.83	1.03	10.75
	2	−1.650	—	—	0.35	—	—	0.79	8.29
	3	—	—	—	—	—	—	—	—
0.39	1	−0.875	−0.850	−0.025	0.77_5	0.57_5	0.74	1.76	9.88
	2	−1.550	—	—	0.67_5	—	—	1.53	8.59
	3	−2.100	—	—	0.95_0	—	—	2.16	12.13
0.63	1	−0.875	−0.840	−0.035	1.50	0.65	0.43	3.40	11.82
	2	−1.525	—	—	1.15	—	—	2.61	9.07
	3	−2.100	—	—	1.20	—	—	2.72	15.28

a) Units: Same as in Table 2. b) Blanks denote not-workable data or drawn-out waves. c) C is in mM (calculated on the basis of total average molecular weight of the oligomer).

both waves are quasi-reversible process. The totally nonreversible character of peak 3 in 0.0013 M TBAI is given by a shift of E_{pc} towards negative potentials by increasing v and by the lack of a peak in the anodic branch of the CV curves at all scan rates (Fig. 3). In 0.1 M TBAI E_{pc_1} shifts towards negative potential at all scan rates whereas E_{pc_2} are found virtually constant with v. The anodic cathodic peak potentials separation (ΔE_p) of <40 mV at lower scan rates (<0.200 $V s^{-1}$) (Table 3) for peak 1 may be accorded with on the basis of Kemula criterion[8] in the support of a quasi-reversible charge-transfer kinetics.# However, the absence of anodic peak for second reduction in 0.1 M TBAI confirms its irreversible nature despite the potential shift. The scan rate-independence of peak 3 with ΔE_p −0.085 V and I_{pa}/I_{pc} ratio around 0.93 suggest that the degree of reversibility in the present instance is considerably high. There is apparently no effect of switching potential (E_λ) on E_{pc_1}; E_{pa_1}, and E_{pc_2}; E_{pa_2}. However, the increase in I_{pa} for both waves when E_λ is less cathodic (−1.5 V) after 0.100 $V s^{-1}$ is due to the availability of reduced material for the required oxidation. It may be noted that the increment in $I_{pa_{1,2}}$ at lower v<0.050 $V s^{-1}$ is not seen. This shows that the reduction material which was initially adsorbed has sufficient time to diffuse in the bulk as the time elapses between the cathodic and anodic wave because of slow scan rate.[9] When the E_λ is made more negative, the significant removal of reduction product of second reduction by the fourth irreversible step may cause smaller I_{pa} (Fig. 3).

The $I_{pc}/v^{1/2}$ vs. $v^{1/2}$ (or $I_{pc}/Cv^{1/2}$ vs. $\log v^{1/2}$) (Figs. 5a and 5b) in both concentrations of TBAI indicates the case where reactant is weakly adsorbed and product is strongly adsorbed at two different values of free energy (ΔG°) of adsorption.[9] The dominant fall in current function with increase of scan rate can be ascribed to the process where reactant initially adsorbed and diffusion of reactant combined cannot provide the material required for the strong adsorption of the product, and consequently all the adsorbed reactant is reduced in the potential region of the pre-peak and the normal diffusion peak diminishes. The small cathodic shift in adsorption pre-peak and normal diffusion peak with increasing scan rate in this case may be due to the partial depletion of reactant during the adsorption process. The decrease in current function and ΔE_p with v (Table 1) denotes the quasi-reversible nature of the concerned peaks. The unprecedented rise in I_{pa}/I_{pc} for peak 1 (Fig. 6) at 0.0013 M TBAI and for peaks 1 and 3 at 0.1 M TBAI (Fig. 6) suggests the presence of chemical reactions preceding the charge transfer reactions (CE mechanism).[10] The only wave which demonstrated a decrease in I_{pa}/I_{pc} value with scan rate (Fig. 6) is peak 2 recorded in supporting electrolyte concentration 0.0013 M (This peak is found irreversible in the concentrated solution of supporting electrolyte 0.1 M). This supports, according to Nicholson and Shain,[11] that the charge transfer is quasi-reversible in the present instance followed by a reversible chemical reaction (EC mechanism). Since peak 2 is irreversible in 0.1 M TBAI, succeeding chemical reaction will have no effect on the nature of the charge transfer. The reaction mechanism based on above discussions could be described in terms of the following reactions:##

$$PTVCl_2 \rightleftharpoons PTVCl + Cl^- \quad \text{(i)}$$

$$(PTVCl)_{soln} \rightleftharpoons (PTVCl)_{adsorbed} \quad \text{(ii)}$$

$$(PTVCl) + e \overset{\text{peak 1}}{\rightleftharpoons} (PTVCl^\bullet) \quad \text{(iii)}$$

$$(PTVCl^\bullet) + e \overset{\text{peak 2}}{\rightleftharpoons} (PTVCl^{\bullet\bullet}) \quad \text{(iv)}$$

#Adsorption is treated as a minor perturbation here, but appears to control much of the electrochemical behavior. A quick glance at Fig. 4 reveals a peak separation much less than 59 mV for the first major couple, suggesting a loosely surface-attached radical species for the reverse polarization.

##Maximum dissociable Cl^- ions in step (i) could be $(n+1)$ Cl^- ions where degree of polymerization (n) is 5; other Cl^- ions remain associated as PTVCl (Charts 1 and 2).

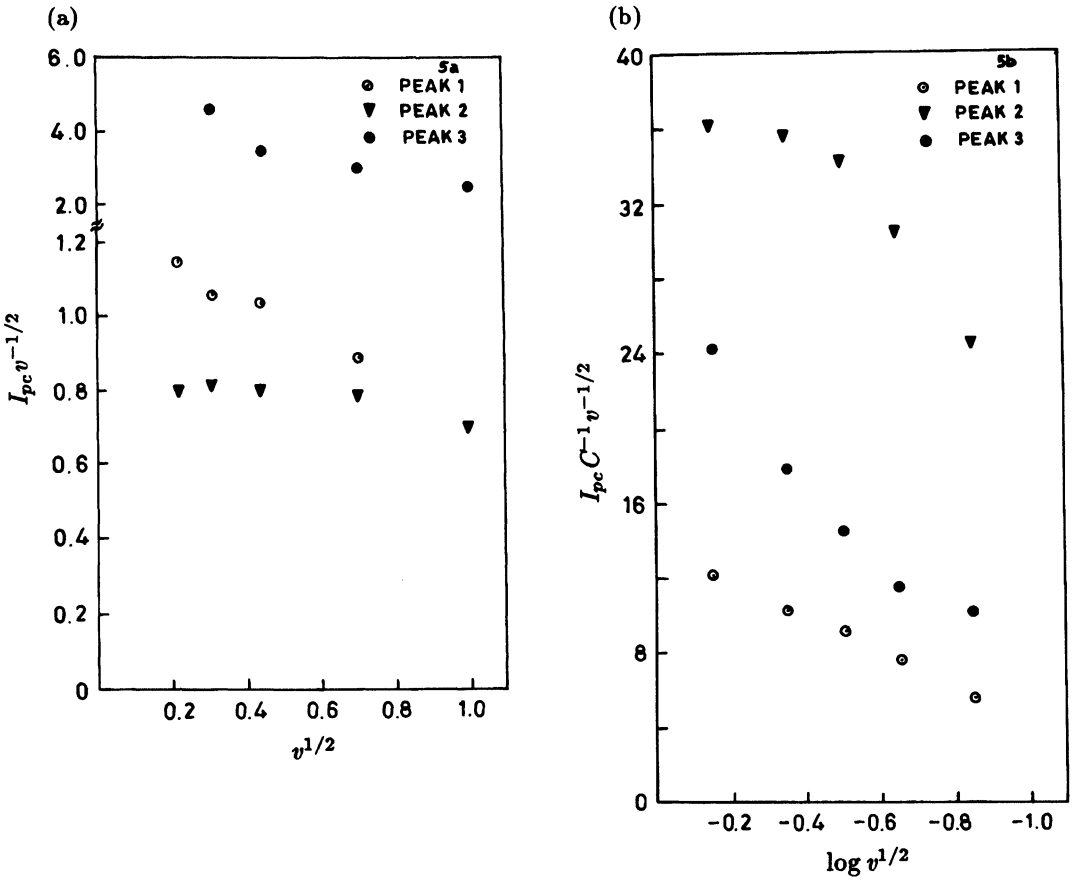

Fig. 5. (a) Variation of current function ($I_{pc}/v^{1/2}$) with scan rate (TBAI 0.1 M). (b) Variation of current function ($I_{pc}/Cv^{1/2}$) with scan rates (TBAI 1.3×10^{-3} M).

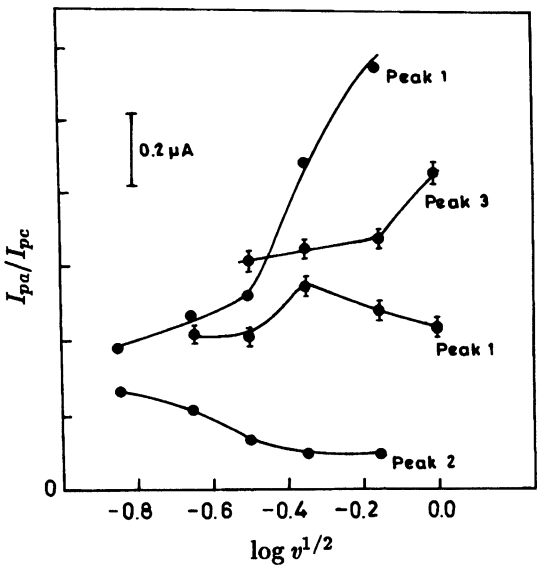

Fig. 6. Variation of I_{pa}/I_{pc} with scan rates (●, 1.3×10^{-3} TBAI, ◖, 0.1 M TBAI).

$$PTVCl^{\bullet\bullet} \rightleftharpoons PTV^{\bullet\bullet} + Cl^- \quad (v)$$

$$PTV^{\bullet\bullet} + e \xrightarrow{peak\ 3} PTV^{\bullet\bullet\bullet} \quad (vi)$$

In the above mechanism weak adsorption of the PTVCl and strong adsorption of $PTVCl^{\bullet}$ in both concentrations of supporting electrolyte may well accord the emergence of 'reversible' pre-peaks $i_{pc'}$, $i_{pa'}$ and 'reversible' post-peaks $i_{pc''}$ and $i_{pa''}$ (Fig. 3) which are clearly observed at higher scan rates. Steps (i) and (v) serves as preceding chemical reactions for peak 1 (both TBAI concentrations) and peak 3 (for 0.1 M TBAI) while step (v) serves as succeeding chemical reaction for peak 2 (0.0013 M TBAI). Steps (iv) and (vi) show total irreversibility in the medium containing 0.1 M TBAI and 0.0013 M TBAI, respectively.

Peak 1 in both concentrations of supporting electrolyte has analogous quasi-reversible behavior. However, the opposite trend that is the irreversibility of peak 2 and reversibility of peak 3 in the high ionic strength medium (0.1 M TBAI) in comparison to those observed (i.e., reversibility of peak II and irreversibility of peak III) in low concentrated medium (0.0013 M) of supporting electrolyte TBAI is quite interesting. This could be presumably attributed to the fast electrode kinetics owing to the electrostatic attraction of the system ($PTVCl^{\bullet\bullet}$) by TBA^+ ions originally adsorbed over Hg drops at higher negative potential. As a consequence $PTVCl^{\bullet\bullet}$ would be taken away for the succeeding reduction efficiently and may not be extricated for oxidation by TBA^+ ions in the reverse scan. Such phenomenalistic effect is apparently being omitted in low concen-

Table 4. Kinetic Parameters Derived from Total Irreversible Cyclic Voltammetric Peak (Peak 3) for $PTVCl_2$ (0.390 $g\,dm^{-3}$) in 1.3×10^{-3} M TBAI at 25 °C

Scan rate	$E_{p/2}$	α_n	b	$k_s\times10^3$	D[a)]	K°_{fh}
$V\,s^{-1}$	V			$cm\,s^{-1}$	$cm^2\,s^{-1}$	$cm\,s^{-1}$
0.100	−1.65	0.34	0.17	3.74	4.76×10^{-4}	5.37×10^{-10}
0.200	−1.70	0.31	0.19	4.56	7.15×10^{-6} [b)]	—
0.500	−1.775	0.29	0.20	5.67	—	—

a) D is obtained polarographically from Cottrell equation and K°_{fh} is calculated from the equation,[11c)]

$$E_{1/2} = -0.2412 + \frac{0.05915}{\alpha_n}\log\frac{1.349K^\circ_{fh}t^{1/2}}{D^{1/2}}.$$

b) D value for $PTVCl_2$ (0.390 $g\,dm^{-3}$) in 0.1 M TBAI from NPP mode (peak 3).

trated TBA^+ ions. The reduction product $PTV^{\bullet\bullet\bullet}$ undergoes electron-pairing and assumes structurally stabilized species which is probably difficult to be oxidized in the reverse scan as demonstrated by the irreversible behavior of peak 3 in 0.0013 M TBAI. The situation is different in highly concentrated medium (0.1 M) of TBAI. In this case free radical stabilization through electron-pairing of $PTV^{\bullet\bullet\bullet}$ is apparently restricted owing to the intermolecular electrostrictional attractions which in turn facilitates the quick oxidation of the reduced product. Further ion-pairing in the structure at higher concentration of TBAI could be also taken into account which disfavors adsorption of the reduction product, if any, in reverse scan. In fact, the instant fall of I_{pa}/I_{pc} values at higher scan rates in 0.1 M TBAI (Fig. 6) may be also due to the skipping of step (i) (i.e. adsorption of reactant) and consequently, the enhancement of cathodic reductions of PTVCl is seen which cut down the $I_{pa'}/I_{pc'}$ values drastically in fast sweep measurements for peak 1.

The kinetic parameters transfer coefficient 'α_n' and standard rate constant 'k_s' for the irreversible reduction (peak 3) of $PTVCl_2$ (0.39 $g\,dm^{-3}$) at HMDE in 0.0013 M TBAI are calculated for different scan rate by the following relationships[11a,11b,11c)] at 25 °C

$$\alpha_n = \frac{1.857\,RT}{F\cdot(E_p - E_{p/2})} \quad (4)$$

$$I_p = 3.01\times10^5 nA\left(2.30\frac{RT}{bF}\right)^{1/2} D^{1/2}CV^{1/2} \quad (5)$$

$$E_p = E_{p/2} - b[0.52 - 0.5\log\left(\frac{b}{D}\right) - \log k_s + 0.5\log v] \quad (6)$$

$$b = \frac{2.303\,RT}{n^F} \quad (7)$$

where I_p=peak current (μA), n=no. of electrons in the reduction, C=concentration (mM), A=electrode area (1.56×10^{-2} cm^2) and b=Tafel coefficient (concentration used here is calculated on the basis of a total average mol wt of the oligomer). The results obtained are presented in Table 4. The comparison of diffusion coefficient ($D=4.76\times10^{-4}$ $cm^2\,s^{-1}$) of $PTVCl_2$ with that of ($D=5\times10^{-6}$ $cm^2\,s^{-1}$) of monomeric methyl viologen is apparently difficult as there is some prevalent migration contribution in the mass transport in the presence of uncompensated resistance of the polyelectrolyte solution with dilute concentration (1.3×10^{-3} M) of the supporting electrolyte. The diffusion coefficient of $PTVCl_2$ in 0.1 M TBAI, however, revealed somewhat comparable values with that of methyl viologen. This reflects an usual polyelectrolytic solvation behavior of intramolecular constriction in DMSO owing to the presence of larger concentration of supporting electrolyte. Furthermore, there is a substantial impact of compensated and uncompensated solution resistance which involves consequently higher currents through the cell due to effective mass transfer in both conditions. This may be the reason for higher D values (Table 4) obtained in 1.3×10^{-3} M TBAI and a comparable value in 0.1 M TBAI despite the larger size of $PTVCl_2$ as compared to methyl viologen.

The overall rate constant for the electrode process (wave 3) is a linear function of electrode coverage (θ) and is the sum of standard rate constant at the bare surface and that at the filmed portion.[12)] The occupied film by the reduction product (i.e., the reactant ($PTV^{\bullet\bullet}$) for successive third reduction), in the present instance, restricts the rate of electron transfer reaction to some extent by partially blocking the electrode surface and the electrode reaction is facilitated primarily at the uncovered fraction ($1-\theta$). In fast sweep voltammetry like CV, the fraction ($1-\theta$) is more available with increase in scan rate (v). This is the reason why 'k_s' in CV has larger value than heterogeneous forward rate constant (K°_{fh}) in DCP-tast mode and moreover exhibits unusual variation with potential scan rate.

The assistance rendered by UGC under COSIST programme is greatly acknowledged.

References

1) C. L. Bird and A. T. Kuhn, *Chem. Soc. Rev.*, **10**, 49 (1981).

2) a) B. B. Prasad, *J. Macromol. Sci., Chem.*, **A22**, 1 (1983); b) B. B. Prasad, *J. Macromol. Sci., Chem.*, **A21**, 1493 (1984); c) L. M. Mukherjee and B. B. Prasad, *J. Macro-*

mol. Sci., Chem., **A16**, 1263 (1981); d) A. Kumar, S. Easo, S. Sundd, and B. B. Prasad, *Ann. Chim. (Rome)*, **83**, 159 (1993); e) B. B. Prasad, *Electrochim. Acta*, **30**, 597 (1985); f) B. B. Prasad, *Bull. Chem. Soc. Jpn.*, **62**, 1269 (1989); g) D. A. Hall and P. J. Elving, *Electrochim. Acta*, **12**, 1363 (1967).

3) B. B. Prasad, S. Easo, and A. Kumar, *Polymer*, in press; *Polym. J.*, **26**, 251 (1994).

4) A. N. Kost and S. I. Suminov, "*N*-Acyl Pyridinium Salts," in "Iminium Salts in Organic Chemistry," ed by H. Böhme and H. G. Viehe, John Wiley and Sons, New York (1979), Part 2.

5) K. B. Oldham and E. P. Parry, *Anal. Chem.*, **42**, 229 (1970).

6) E. P. Parry and R. A. Osteryoung, *Anal. Chem.*, **37**, 1634 (1965).

7) E. P. Parry and K. B. Oldham, *Anal. Chem.*, **40**, 1031 (1968).

8) W. Kemula, Z. Kublik, and A. Axt, *Rocz. Chem.*, **35**, 1009 (1961).

9) R. H. Wopschall and I. Shain, *Anal. Chem.*, **39**, 1514 (1967).

10) R. S. Nicholson and I. Shain, *Anal. Chem.*, **36**, 706 (1964).

11) a) E. Gileadi, E. Kirova-eisner, and J. Penciner, "Interfacial Electrochemistry," Adison-Wesley, London (1975), p. 373; b) Z. Galus, "Electroanalityczne Metody Wyznaozama Stalych Fizykochmicznych," PWN, Warsaw (1979), p. 224; c) L. Meites, "Polarographic Techniques," 2nd ed, Wiley Intersciences, New York (1965), pp. 224, 236, 240, 244, and 518.

12) A. J. Bard and L. R. Faulkner, "Electrochemical Methods," John Wiley and Sons, New York (1980), pp. 539 and 569.